

AD-A228 788

2

CWP-090P
October, 1990



A COMPUTER IMPLEMENTATION OF
2.5D COMMON SHOT INVERSION

by

Wenjie Dong,^{*†} Mark Jeffrey Emanuel,^{*††}
Phillip Bording,^{†††} and Norman Bleistein^{*}

Partially supported by the Office of Naval Research
and partially supported by the Consortium Project on
Seismic Inverse Methods for Complex Structures
at the Center for Wave Phenomena

Present addresses:

[†]ERL/MIT
Room E34-342
42, Carleton Street
Cambridge, Massachusetts 02142

^{††}Chevron Exploration & Production Services
P.O. Box 1635
Houston, Texas 77251-1635

^{†††}Minnesota Supercomputer Center, Inc.
5510 South Yale
Suite 301
Tulsa, Oklahoma 47135

^{*}Center for Wave Phenomena
Department of Mathematical and Computer Sciences
Colorado School of Mines
Golden, Colorado 80401

DISSEMINATION STATEMENT A
Approved for public release
Distribution Unlimited

DTIC
ELECTE
NOV 07 1990
S D 3 D

INTRODUCTION

The purpose of this paper is to describe a computer implementation of a two-and-one-half (2.5D) dimensional constant density prestack inversion formalism with laterally and depth dependent background propagation speed. We refer to this inversion procedure as "Kirchhoff inversion" because of the striking similarity between this method and Kirchhoff migration in a variable background medium. The major difference is a spatial weighting derived from the inversion theory.

In this implementation, this medium is made up of constant velocity layers with curved interfaces, although this specialization is not a requirement of the theory. The origins of this approach to seismic inversion can be found in the work of Cohen and Bleistein (1979), Bleistein and Gray (1985), and Cohen and Hagin (1985). Beylkin (1985) proposed a method of operator inversion that generalizes the results of those papers. An extension of that theory, consistent with the earlier work, was developed in the papers of Cohen, Hagin and Bleistein (1986); and Bleistein, Cohen and Hagin (1987). The extension revises the Beylkin inversion operator in two ways. The first modification provides a reflector map instead of a velocity model, with the peak amplitude on each reflector being proportional to the geometrical optics reflection coefficient. This work has its origins in a series of papers: Bojarski (1967, 1968), Mager and Bleistein (1978), and Cohen and Bleistein (1979). This modification provides a quantification for the more abstract construct of a "wavefront set" of the pseudo-differential operator approach to inverse scattering following Beylkin (1985). This modification is a matter of necessity for seismic data, which tends to be high frequency data for the length scales of the seismic experiment. From such band-

limited data, it is not practical to extract information about the velocity (medium parameter) field itself, but only about the "discontinuity surfaces" — the reflectors — of those parameters.

The second modification provides a 2.5D inversion. That is, it allows for the processing of a line of data to produce a two dimensional reflector map with amplitudes that approximate the effect of the out-of-plane spreading of the response to a three dimensional point source. The method assumes that the subsurface has two dimensional variation only, with the data line being a dip line of the subsurface.

The inversion operator presented in these papers is based on the Born approximation for the wave upward scattered from the inhomogeneities in the earth. However, an analytical proof of the validity of the inversion formalism as applied to Kirchhoff-approximate data has been presented in Bleistein (1987a, 1987b, 1989). This proof partially overcomes the "small perturbation" constraint of the motivating Born approximation. The proof shows that if the background medium above a reflector is known (or the background is close to the true medium above the reflector) then the reflector will be properly positioned (approximately, for a close background). Furthermore, the peak output on the reflector is linear in the angularly dependent geometrical optics reflection coefficient, from which it follows that the change in earth parameters across the reflector being imaged need not be small.

As an alternative to the use of the Born approximation, one can start with the Kirchhoff approximation for a single reflector and develop an inversion operator based on this model. This method leads to the same inversion formalism, as might be expected by the method of proof described above. An implementation of this

approach for common offset inversion is presented in Sullivan and Cohen (1987). Docherty (1987a, 1987b) also applied this approach to 2.5D zero offset inversion in a medium comprised of many layers. The first author of this paper used the same approach to confirm the inversion for prestack common shot 2.5D inversion (Dong, 1989, Dong and Bleistein, 1989) and to verify equation (50) in Bleistein, Cohen and Hagin (1987) for this case. The computer implementation was then developed using Docherty's zero-offset inversion code as a point of departure. For details of the derivation of the inversion operator, the reader is referred to those references.

The computer implementation was tested on ray-theoretic data synthetically generated with Docherty's (1987a) *CSHOT* program. In addition, tests were carried out on physical model data. Physical model data are useful for testing and comparing seismic data imaging techniques (migration or inversion). The physical model data are actual recorded wavefields and contain all wave effects including lateral waves, near field effects, mode conversions, and diffractions. Seismic data modeling and imaging methods are based on a theory that incorporates simplifying assumptions about the wavefield. If an imaging procedure is based on the same theory as the modeling procedure, the imaging procedure is merely the inverse of the modeling procedure. While this is an advisable first test on an inversion formalism, the imaging might work perfectly on synthetic data from the modeling, but might not work on field data. Beyond numerically generated data, physical model data provides the next level of test; the data are real wavefields. Since the models are simpler than the real earth and the physical parameters are known, physical model data can be used to verify imaging techniques.

Our physical model data was generated at the Seismic Acoustic Laboratory at the University of Houston under support of Marathon Oil Company, who uses such physical model data to evaluate imaging (migration) processing by contractors. Since the result is known beforehand, this can be input as the migration background velocity function. The migration techniques can be compared independent of the velocity analysis. Marathon donated a physical model data set to the Center for Wave Phenomena so that we might try our inversion on the data. The model is structurally complicated enough to warrant prestack inversion. Furthermore, the model was sufficiently two dimensional to make the application of Dong's code to this data practical. That application was carried out by the second author of this paper. An extensive discussion of the analysis of this data, including a search for mode converted waves and lateral waves, can be found in Emanuel (1989a, 1989b).

Parameter estimation for the synthetic data set showed errors of about 7%. Parameter estimation for the experimental data was less successful, partially due to problems with amplitude control in the original experiment. Both data sets suffered from the limited aperture of the common shot data, which degrades amplitude accuracy, thereby suggesting that a common offset inversion might be more useful for parameter estimation. Tests with a common offset inversion program are now in progress and will be reported in a future paper. Earlier tests on wide aperture synthetic data with fine sampling produced satisfactory amplitude estimates and

convinced us that the theory is valid.

THE CXZCS ALGORITHM

For a 2.5D acoustic model comprised of constant velocity layers, separated by arbitrary smooth interfaces, and for a flat observation surface, the common shot inversion algorithm is (Dong [1989], equation [3.5.5])

$$B(x) = \frac{4\pi\sqrt{2}}{c(x)} \int d\xi K(x_s, \xi, x) D_m(\tau_s + \tau_r, \xi), \quad (1)$$

where

$$K(x_s, \xi, x) = \frac{\sqrt{\sigma_s + \sigma_r} \sqrt{\cos\beta(x_s) \cos\beta(\xi)} \sqrt{\partial\beta(\xi)/\partial\xi}}{T(x_s, x) T(\xi, x) \sqrt{\partial\beta(x_s)/\partial\xi}}, \quad (2)$$

$$D_m(t, \xi) = \frac{1}{A_f} [\text{Re} - \text{Im}] \int_0^\infty df \sqrt{f} e^{-2\pi i f t} D(f, \xi). \quad (3)$$

The variables in these formulas, and those immediately following, are defined in Table I. Except for the factor, A_f , this is just the "reflectivity function" called $\beta_1(x)$ in Bleistein (1987a). (We avoid the use of β for reflectivity functions here because of the use of this variable for incidence angles on the upper surface.) The introduction of the scale A_f , means that in the neighborhood of a reflector, the function $B(x)$ has the approximation,

$$B(x) \approx R(x, \theta) \gamma_0(x) h(x). \quad (4)$$

Table I	
$R(x, \theta)$	angularly dependent geometrical optics reflection coefficient at output point x .
$\gamma_0(x)$	band-limited wavelet, or singular function, of unit height.
$D(f, \xi)$	Fourier transform of time trace at receiver location ξ .
$D_m(t, \xi)$	Modified time section defined in (3).
$\cos\theta$	cosine of the incident angle at reflection point.
$c(x)$	background propagation speed at location x .
$\sigma_s; \sigma_r$	ray trace running parameter from output point to source and receiver, respectively.
$\beta(x_s), \beta(\xi)$	angles between ray and upward vertical at x_s and ξ .
$\partial\beta(\xi)/\partial\xi, \partial\beta(x_s)/\partial\xi$	in-plane ray spreading factors at location ξ and x_s .
τ_s, τ_r	traveltimes between output point at x and source at x_s or receiver at ξ , respectively.
$T(x_s, x), T(\xi, x)$	product of transmission effects at each interface between output point x and source at x_s or receiver at ξ (see reference, equation 3.5.2).
\sqrt{f}	phase compensator due to 2.5D (\sqrt{if}) is achieved through this multiplier and the use of Re - Im combination of half inverse transform.
A_f	Area of bandpass filter applied to $D(f, \xi)$.

In this equation, $h(x)$ is a slowly varying function of x , on the scale of wavelengths, with $h(x) = 1$ on the reflector, itself. The other new variables here are also defined in Table I.

From these equations alone, one cannot estimate the change in propagation speed across a reflector. It is necessary to determine the distinguished value of θ in $R(x, \theta)$ to extract information about the propagation speed of the lower medium. With little extra effort, the program also outputs the angularly dependent reflection coefficient multiplied by $\cos \theta$ on the peak of the singular function. The formula for this second inversion is

$$B_c(x) = \frac{4\pi\sqrt{2}}{c(x)} \int d\xi K_c(x_s, \xi, x) D_m(\tau_s + \tau_r, \xi) , \quad (5)$$

where

$$K_c(x_s, \xi, x) = K(x_s, \xi, x) c(x) |\nabla(\tau_s + \tau_r)| / 2 , \quad (6)$$

with the new variables again defined in Table I. Except for the factor, $c(x)/2A_f$, this is the reflectivity function, $\beta(x)$, in Bleistein (1987a). In the neighborhood of a reflector,

$$B_c(x) \approx R(x, \theta) \cos \theta \gamma_0(x) h(x) . \quad (7)$$

It can now be seen that the ratio of the peak values of the two outputs, $B_c(x)/B(x) \approx \cos \theta$, and then either of the outputs can be used to estimate the change in propagation speed across a reflector from the dependence of the reflection coefficient on the two propagation speeds and θ :

$$R(\mathbf{x}, \theta) = \frac{\frac{\cos \theta}{c(\mathbf{x})} - \left[\frac{1}{c_+^2(\mathbf{x})} - \frac{\sin^2 \theta}{c^2(\mathbf{x})} \right]^{1/2}}{\frac{\cos \theta}{c(\mathbf{x})} + \left[\frac{1}{c_+^2(\mathbf{x})} - \frac{\sin^2 \theta}{c^2(\mathbf{x})} \right]^{1/2}} \quad (8)$$

In this equation, $c_+(\mathbf{x})$ is the propagation speed below the reflector to be determined from this function and the peak value of $B(\mathbf{x})$, for example, on the reflector.

In Bleistein (1987b), the extension of this theory to the variable density case is discussed. If the background density is constant, equations (1) and (5) still apply and we need only interpret the output in terms of the variable density geometrical optics reflection coefficient. If the background density on the upper surface is not constant, then one need only modify those formulas by a multiplier of $\sqrt{\rho(\mathbf{x}_s)/\rho(\mathbf{x}_g)}$, with $\rho(\mathbf{x})$ the background density. Now it is necessary to estimate the changes in two medium parameters across each reflector. At least two common shot inversions imaging the same point on a reflector, with different incidence angles, θ , are necessary in this case to estimate parameter changes. Parsons (1986) further extended this scalar theory by interpreting the output as a PP reflection coefficient in an elastic medium. Now, at least *three* common shot inversions imaging the same point on a reflector with different incidence angles, θ , are necessary to estimate parameter changes. In practice, all outputs imaging the same point are used to minimize the effects of noise.

The program *CXZCS* implements equations (1) and (5) above. The filtering operation that produces the modified data $D_m(t, \xi)$, described by equation (3), is carried out by a separate program. This filtering step is independent of the inversion process and does not have to be redone to test different background models. This step

is carried out using a fast Fourier transform routine, producing $D_m(t, \xi)$ on a uniform grid in t . The value $D_m(\tau_s + \tau_r, \xi)$, needed in equations (1) and (5), is then approximated by three point interpolation.

The basic CXZCS algorithm (without interpolation) is summarized below:

For each output trace
 For each depth z on the output trace
 For each receiver ξ
 Trace rays from x to ξ
 Calculate τ 's, β 's, σ 's, $\partial\beta$'s
 Weight modified data at time $\tau_s + \tau_r$ and sum into output at x
 Next receiver
 Multiply output at x by constants
 Next output depth
 Write output trace to disk
Next output trace

Each output trace in the depth section is written as a single record and, as above, has no header.

RAYPATH CALCULATIONS

The raypath calculation algorithm in CXZCS is the same as in Docherty (1987a). The raypath between output points and receivers on the observation surface are calculated using continuation in both interfaces and receivers. That is, a first ray path trajectory from source to a first output point to receiver is determined for flat interfaces. Then, continuation in the interface shapes is used to determine the ray trajectory for the actual interfaces. For each continuation, here and in the following,

Newton's method is used to determine the new trajectory. The trajectory from the source to the output is determined this way, as well. Continuation in receiver position is then used to determine the ray paths to all receivers.

INTEGRATION RANGE SPECIFICATION AND INTERPOLATION

To image a point on a reflector we must insure that the specularly reflected energy from that point emerges within the range of integration in equations (1) and (5). If the dip of the reflector varies across the section, it is likely that the required range of integration will also vary. To be safe, one usually specifies the range of the integration to include all the receivers used in the experiment. This can be costly and may lead to difficulties and pathologies associated with ray tracing.

For efficiency, this program allows the user to define different inversion panels. In each panel, the integration range can be defined differently to avoid rays that do not give contributions to the integration. This requires some a priori knowledge of the true earth structure.

Our knowledge of true earth is expressed in the trial depth model that we input to the program. Given the shot and receiver positions, this model serves as our guide in selecting the integration range. At different output points, we simply choose the limits of integration (in terms of receiver numbers) to be used in the integrals in equations (1) and (5). At output points between specified output locations the program adjusts those limits so that the integration range varies smoothly across the section. This is especially useful in regions of complex geological structure.

The geometry of the seismic experiment has to be given before the integration range can be specified. In *CXZCS*, all receivers are located on a flat observation surface, although the theory allows for a variable height upper surface. All the receiver locations correspond to the trace locations of the data. The user specifies the *number* of receivers, the *location* of the *first* receiver, and the *spacing* between them (therefore, uniform spread only). The inverted (migrated) depth section is a rectangular grid located somewhere within the trial model.

CXZCS correctly treats geometrical caustics, the bow-tie-like reflections that appear on some shot profiles. In *CXZCS*, every possible ray is traced from the output point to every receiver. This decomposes the bow-tie reflections into outputs on different locations along that interface. Therefore, the inversion outputs from the bow-tie-like reflections are still true amplitude. On the other hand, *CXZCS cannot* correctly treat caustics of the Green's function of the background medium. In that case, we would have to account for the phase change in the inversion. This restriction constrains the user's choice of trial depth models. The theory can accommodate this anomaly, but this first program was not designed to deal with it.

There are other considerations in the code that are worth mentioning here. The first is the antialiasing filter. Spatial aliasing of seismic data is caused by insufficient sampling. Receiver spacing and temporal bandwidth determine the maximum emergence angle of rays at the upper surface beyond which data will be aliased to lower transverse wave number. We define θ_a as the critical angle of emergence at the upper surface, beyond which information is aliased; θ_a is defined by

$$\theta_a = \sin^{-1} \left[\frac{c}{2f_{\max} \Delta \xi} \right] \quad (9)$$

(Bleistein, Cohen and Hagin [1985]). Here, f_{\max} is the maximum frequency in the data, c is the near surface layer velocity, and $\Delta \xi$ is the receiver spacing. For rays whose emergence angle is greater than θ_a , we set the amplitude contribution of these rays to zero. before inversion.

The second consideration is the sampling rate of output depth. We take a sinc function as a prototypical band-limited delta function as might appear in the output of the inversion. We then require that the sampling rate in depth be such that there are four sample points in the interval of the main lobe of a sinc function with the same bandwidth as the given signal of the filtered data. Therefore, if Δz is the sample interval, one can show that

$$\Delta z = \frac{c}{8(f_{\max} + f_{\min})} \quad (10)$$

(See Dong [1989] for a discussion.) We remark also that the first zero of the sinc function away from its maximum belongs to the upper medium. That is, where the background medium changes, we process with the upper medium propagation speed for sufficient depth to include the main lobe of the sinc function. For deeper points, rays and traveltimes are calculated with the background interface in place. The range below a discontinuity of the background for which we use the upper medium propagation speed is

$$\Delta z_1 = \frac{c}{2(f_{\max} + f_{\min})} \quad (11)$$

The algorithm we have outlined so far calculates raypaths from every output point up to receivers within a specified range on the observation surface. Unfortunately, for large data sets the time spent on ray tracing can be excessive and may account for as much as 99% of the total run time. The interpolation procedures we describe next were introduced by Docherty (1987a) in an effort to reduce the cost of the ray tracing. He found that in most cases accurate images and amplitudes could be obtained from only a sparse set of ray path calculations, thus reducing the run time considerably. Typically, such calculations will be carried out only for every fifth (or tenth) receiver point and for each fifth (or tenth) output point both laterally and vertically, thereby saving a factor of 125 to 1000 on the ray path calculations. Some care is necessary near the "top" of the (pseudo) hyperbola of the traveltime curve for a particular output point. Except for that, interpolation is equivalent to replacing the given background model by a nearby model. Since the background is an approximation, at best, a nearby approximation would seem not to be a serious compromise for the CPU time that is gained. For further details, the reader is referred to Dong (1989).

SYNTHETIC EXAMPLE

This example demonstrates the inversion on a syncline consisting of four interfaces. The shot is located at the middle of the receiver array. Sample ray paths and the shot record are displayed in Figures 1 and 2, respectively. In the latter, we can see the bow-tie-like reflection from the lowest interface. The inversion result is

shown in Figure 3. We can see that for portions that rays have illuminated, the inversion result is close to the original model. Note that the bow-tie and attendant phase shifted source signature have been successfully unravelled by this processing. All the tails on the inversion section are due to the arbitrary truncation of the data and the impulse response of the inversion operator. Also, we note that for the portion poorly illuminated by rays, the inversion result is weak. Therefore, we can not expect to determine the reflection coefficient in this part of the output. Even in the region of illumination, it is not clear that the output comes from a sufficient input aperture to provide good numerical accuracy (Cohen, 1989). Estimates in regions of strongest illumination on the syncline exhibit errors up to 7% in the change in propagation speed.

THE MARATHON MODEL

The data were collected for Marathon Oil Company at the Seismic Acoustics Laboratory at the University of Houston in a water tank over a block model. Figure 4 is a cross-section of the model. The model varies only slightly in the y - (out-of-plane) direction so that the 2.5D assumption used for deriving the inversion operators in equations (1) and (5) are reasonable for these data. The top layer was water. The other layers were various epoxy resins. The dimensions in Figure 4 are labeled in scaled feet; the original tank model was only about three feet wide. For brevity, we use feet and seconds instead of scale feet and scale seconds in the discussion below.

The data consist of 290 shot records. There were 48 receivers in an end-on spread. The receivers were to the right of the shot. The near receiver offset was 800 feet and the receiver spacing was 80 feet. The far receiver offset was, therefore, 4560 feet. The shot spacing was also 80 feet. The first shot was located at $x = 0$ feet and the last was at $x = 23200$ feet. The shots and receivers were at depth $z = 0$ feet shown in Figure 4. This is not the water surface though. The shots and receivers were submerged sufficiently so that no reflections from the water surface were recorded. For each shot, two seconds of data were recorded, sampled at 4 ms.

Figure 5 is a sample shot record from these data. AGC has been applied to this record so that more events are visible. The shot location is $x = 2000$ feet and the receiver spread extends from $x = 2800$ to $x = 6560$ feet. The earliest event is the direct wave. The first curved event is the water bottom reflection. The next two events are reflections from the second and third interfaces. The strong event near 1.45 seconds is a reflection from the model bottom. The reflection from the sawtooth interface does not produce an easily identifiable event on this record.

The data have been inverted three times with different parameters.

First Marathon inversion

As with migration, inversion requires a reference velocity field. The velocities used are the exact velocities shown in Figure 4. The interfaces in the derived background model are located nearly in the same positions as the interfaces in Figure 4. Differences occur where the cubic spline fit to the control points causes unwanted bumps on the interfaces. The most severe of these occurs on the down thrown side of

the fault cutting the third interface.

For each shot record, the inversion routine produced 48 output depth traces. The first output trace is located at the shot position. The trace separation is 160 feet. Each trace has 301 samples. The depth sampling rate is 40 feet. For each shot record, the inversion produced an image of the subsurface in the rectangular region from 0 to 12000 feet deep and from the shot location to 7520 feet right of the shot location.

The traveltimes and amplitude functions required by the inversion formula are computed by ray tracing from the output point to the source and to the receivers. Rays were not, however, traced to every output point and every receiver. Instead, rays were traced from each depth point on every fifth output trace and to every fifth receiver. The traveltimes and amplitude functions were interpolated from the values obtained by the ray tracing.

Figure 6 is the inversion of the shot record shown in Figure 5. (Note that Figure 5 shows the shot record after AGC. The inversion is applied to the ungained record.) The inversion is a partial image of the subsurface. Shallower than 1000 feet is noise from the direct arrival. The events at 3000 feet, 4500 feet, and 6300 feet are images of the first three interfaces. The event at 11200 feet corresponds to the model bottom. The fourth reflector, the sawtooth, is faint and located at a depth of 9000 feet and distance of 6000 feet.

An inversion similar to Figure 6 is obtained for all 290 shot records. Each yields a different partial image of the subsurface. The inversions are sorted on the output trace location and stacked to form a full image of the subsurface. Figure 7 is a stack

of all the individual shot inversions. Since the amplitudes are only significant in the individual shot inversions and not the stacked section, AGC has been applied so that all reflections are visible. All reflectors are located correctly including all teeth of the fourth reflector. There are some shortcomings in the inversion.

The first problem is that the steep flanks of the dome are not imaged well. To understand why, consider an experiment in a constant velocity medium with a single reflector and a single source and receiver. The envelope of all reflectors having the same reflection time is the familiar reflection ellipse with the source and receiver at the foci. If the reflector has zero dip, the specular point lies below the midpoint of the source and receiver. As the reflector dip increases, the specular point moves farther up dip and laterally away from the midpoint. Consequently, imaging in a region near the source and receiver, as with this particular example inversion, discriminates against steep dips.

Another problem with the inversion is a phase reversal on the down thrown side of the fault cutting the third interface. There is also a streak of noise extending below this phase reversal. The phase reversal and the noise beneath it are due to the bump on the input model mentioned earlier. The next two inversions were performed to try to remedy these shortcomings.

Second Marathon inversion

For the second example inversion of the Marathon data, several parameters were changed. The inversion output for each shot consisted of 300 traces spaced at 80 feet. This covers the entire model rather than the limited portion of the first inversion.

Recorded energy from all dips should be imageable. The background velocity model was also changed; the velocities were the same but the interfaces have been changed by reducing the number of control points on the interfaces. Consequently, the interfaces did not have the extraneous bumps that the previous model had. The remaining parameter changes concerned the traveltimes and amplitude function interpolation. Rays were traced from each depth point on every other output trace to every other receiver. This was done to achieve as accurate amplitude as possible. The second inversion of all shot records took 3.5 times as much CPU time as the first inversion.

Inversions from all 290 shot records were stacked to form a complete image of the model. The image is shown in Figure 8. Compared to Figure 7, there are some improvements and also some disappointments. As expected, the steep flanks of the dome are better imaged. The phase reversal in the third interface was also removed. There also appears to be a fault plane reflection on the third interface.

The main disappointment from this inversion is the large degree of *migration smile* noise. Migration smiles occupy more area in the shot inversions than the reflector images do. This results in many more noise traces being stacked than signal traces. Although the reflector images (signal) are higher order than the noise, the large quantity of noise traces being stacked can bring the noise to the same level as the signal. The noise has nearly obliterated the fifth tooth in the fourth (sawtooth) interface. Selective windowing of the shot inversions before stacking can reduce the noise level in the final image.

Third Marathon inversion

A third inversion with CXZCS was carried out on a Cray 2 at the Minnesota Super Computer Center. The major objective of this inversion was to see the effect of replacing the sharp velocity contrast across the third interface with two thin layers (one wavelength at minimum frequency). The result is shown in Figure 9. The salt flanks (in a region in which the background velocity was the same as in the previous inversions) and the fault block in the third interface are well imaged. Unfortunately, there is no improvement on the imaging of the sawtoothed structure as we had hoped with this *smoother* background. Ray tracing from the neighborhood of the sawtoothed structure below and to the right of the fault block suggests severe scattering of energy from this region. We believe that this is what we are seeing in the breakup of the image in this region.

The inversion operator delays introduction of a new interface in the background velocity until three wavelengths below that interface. We do this because the theory requires the imaging of each reflector in the background of the *upper medium*. To test this, we replaced the background with one in which the propagation speeds were kept constant below the second interface. In this case, we expect that the image of the third interface should be as in Figure 9, with deeper images degraded. The output in Figure 10 confirms this expectation.

Parameter determination

Parameter estimation studies were carried out with only limited success. There were difficulties because the source was directional and not zero phase. There were

also problems because common shot data sets tend not to be wide enough to give accurate numerical output; common offset inversion would be better for this purpose. This problem increases with depth. Furthermore, the medium was elastic; an acoustic theory, even with variable density, does not account for energy lost to mode conversion, thus further narrowing the useful aperture of the data for parameter estimation. The parameter that seemed to be least affected by these problems was $\cos\theta$, since this uses a ratio of inversion outputs, in which the errors shift the numerator and the denominator in the same direction. For details, see Emanuel (1989a). Certainly, more research needs to be done on this aspect of the theory.

CONCLUSIONS

Common shot, $c(x,z)$, prestack Kirchhoff inversion has been demonstrated to image reflectors. It also provides a means for parameter estimation with limited success (Parsons, 1986) for field data.

For the Marathon physical model data set presented here, the reflectors were also successfully imaged. We have shown that the inversion parameters may be chosen to better image the steep flanks of the shallow dome or the deeper sawteeth. Both, however, may be optimized if care is taken to minimize stacking of noise. The kinematics of the inversion compare favorably to other migrations of the data. More research is required on using this method for computing changes in medium

parameters from output amplitude.

ACKNOWLEDGMENTS

The author gratefully acknowledges the support of the Consortium Project on Seismic Inverse Methods for Complex Structures at the Center for Wave Phenomena, Colorado School of Mines. Consortium members are: Amerada Hess Corporation; Amoco Production Company; ARAMCO; ARCO Oil and Gas Company; BP Exploration Inc.; Chevron Oil Field Research Company; Conoco, Inc.; Exxon Production Research Company; GECO; Marathon Oil Company; Minnesota Supercomputer Center Inc.; Mobil Research and Development Corp.; Oryx Energy Company; Phillips Petroleum Company; Shell Development Company; Texaco USA; UNOCAL; and Western Geophysical. This project was also partially supported by the Office of Naval Research.

REFERENCES

- Beylkin, G., 1985, Imaging of discontinuities in the inverse scattering problem by inversion of a causal generalized radon transform: *J. Math. Phys.*, **26**, 99-108.
- Bleistein, N., 1987a, On the imaging of reflectors in the earth: *Geophysics*, **52**, 931-942.
- Bleistein, N., 1987b, Kirchhoff inversion for reflector imaging and sound speed and density variations: Presented at the EAEG/SEG Workshop on Deconvolution and Inversion, Rome, Italy.

- Bleistein, N., 1989, Large wave number aperture limited Fourier inversion and inverse scattering, *Wave Motion*, **11**, 113-136.
- Bleistein, N., and Cohen, J. K., 1990, Stacking of narrow aperture common shot inversions: *SIAM J. Appl. Math*, **50**, no. 2, 569-594.
- Bleistein, N., Cohen, J. K., and Hagin, F. G., 1985, Computational and asymptotic aspects of velocity inversion: *Geophysics*, **50**, 1253-1265.
- Bleistein, N., Cohen, J. K., and Hagin, F. G., 1987, Two-and-one-half dimensional Born inversion with an arbitrary reference: *Geophysics*, **51**, 26-36.
- Bleistein, N., and Gray, S. H., 1985, An extension of the Born inversion method to depth dependent reference profile: *Geophysical Prospecting*, **33**, 999-1022.
- Bojarski, N. N., 1967, Three dimensional electromagnetic short pulse inverse scattering: *Spec. Proj. Lab. Rep.*, Syracuse Univ. Res. Corp., NY.
- Bojarski, N. N., 1968, Electromagnetic inverse scattering theory: *Spec. Proj. Lab. Rep.*, Syracuse Univ. Res. Corp., NY.
- Cohen, J. K., 1989, Aperture for Kirchhoff inversion: Center for Wave Phenomena Research Report number CWP-079.
- Cohen, J. K., and Bleistein, N., 1979, Velocity inversion procedure for acoustic waves: *Geophysics*, **44**, 1077-1085.
- Cohen, J. K. and Hagin, F. G., 1985, Velocity inversion using a stratified reference: *Geophysics*, **50**, 1689-1700.
- Cohen, J., Hagin, F., Bleistein, N., 1986, Three-dimensional born inversion with an arbitrary reference: *Geophysics*, **51**, 1552-1558.

- Docherty, P., 1987a, Ray theoretical modeling, migration and inversion in two-and-one-half dimensional layered acoustic media: Ph.d. thesis, Colo. Sch. of Mines.
- Docherty, P., 1987b, Two-and-one-half dimensional poststack inversion: 57th Ann. Internat. Mtg. Soc. Expl. Geophys., Expanded Abstracts, 564-565.
- Dong, W., 1989, Finite difference ray tracing and common shot inversion: M.Sc. thesis, Colo. Sch. of Mines.
- Dong, W., and Bleistein, N., 1989, Common-shot inversion in $c(x,z)$ media: 59th Ann. Internat. Mtg. Soc. Expl. Geophys., Expanded Abstracts, 928-931.
- Emanuel, J., 1989a, Common shot, prestack inversion of physical model seismic data: M.Sc. thesis, Colo. Sch. of Mines.
- Emanuel, J., 1989b, Common shot, prestack inversion of physical model seismic data: 59th Ann. Internat. Mtg. Soc. Expl. Geophys., Expanded Abstracts, 1332-1335.
- Gray, S. H., 1986, Efficient traveltimes calculations for Kirchhoff migration: Geophysics, **51**, 1685-1688.
- Mager, R. D., and Bleistein, N., 1978, An examination of the limited aperture problem of physical optics inverse scattering, IEEE Trans. Ant. & Prop., **AP- 25**, 695-699.
- Parsons, R. K., 1986, Estimating reservoir mechanical properties using constant offset images of reflection coefficients and incident angles: 56th Ann. Internat. Mtg. Soc. Expl. Geophys., Expanded Abstracts, 617-620.
- Schneider, W. A., 1978, Integral formulation for migration in two and three dimensions: Geophysics, **43**, 49-76.

Sullivan, M. F. and Cohen, J. K., 1987, Prestack Kirchhoff inversion of common-offset data: *Geophysics*, **52**, 745-754.

Sumner, B., 1988, Asymptotic solutions to forward and inverse problems in isotropic elastic media: Doctoral thesis, Center for Wave Phenomena Research Report number CWP-075.

FIGURE CAPTIONS

- FIG. 1: Syncline model and ray paths. Upper layer velocity is 5000 ft/sec; increment is 1000 ft/sec in each layer. Note: horizontal and vertical scales of plot are not equal.
- FIG. 2: The common shot data generated for the model of Figure 1. Power gain was used for this display.
- FIG. 3: The single shot inversion result of the data in Figure 2.
- FIG. 4: Marathon tank model with given background velocities. These are scaled variables.
- FIG. 5: Sample shot record from the Marathon data. The shot location is $x = 2000$ ft. The receivers extend from $x = 2800$ ft. to $x = 6560$ ft. AGC has been applied for display.
- FIG. 6: Shot inversion of shot record shown in Figure 5. Reflectors are partially imaged.
- FIG. 7: Stack of inversions of all shot records. AGC has been applied.
- FIG. 8: Stack of second inversions of all shot records. Migration noise is greater than in Figure 12 but steeper dips are imaged better. AGC has been applied to the stack.
- FIG. 9: Stack of third inversions of all shot records.
- FIG. 10: Stack of third inversions with background velocity kept constant below the second interface. Compare image of third interface here with the image in Figure 9.

Model and Rays

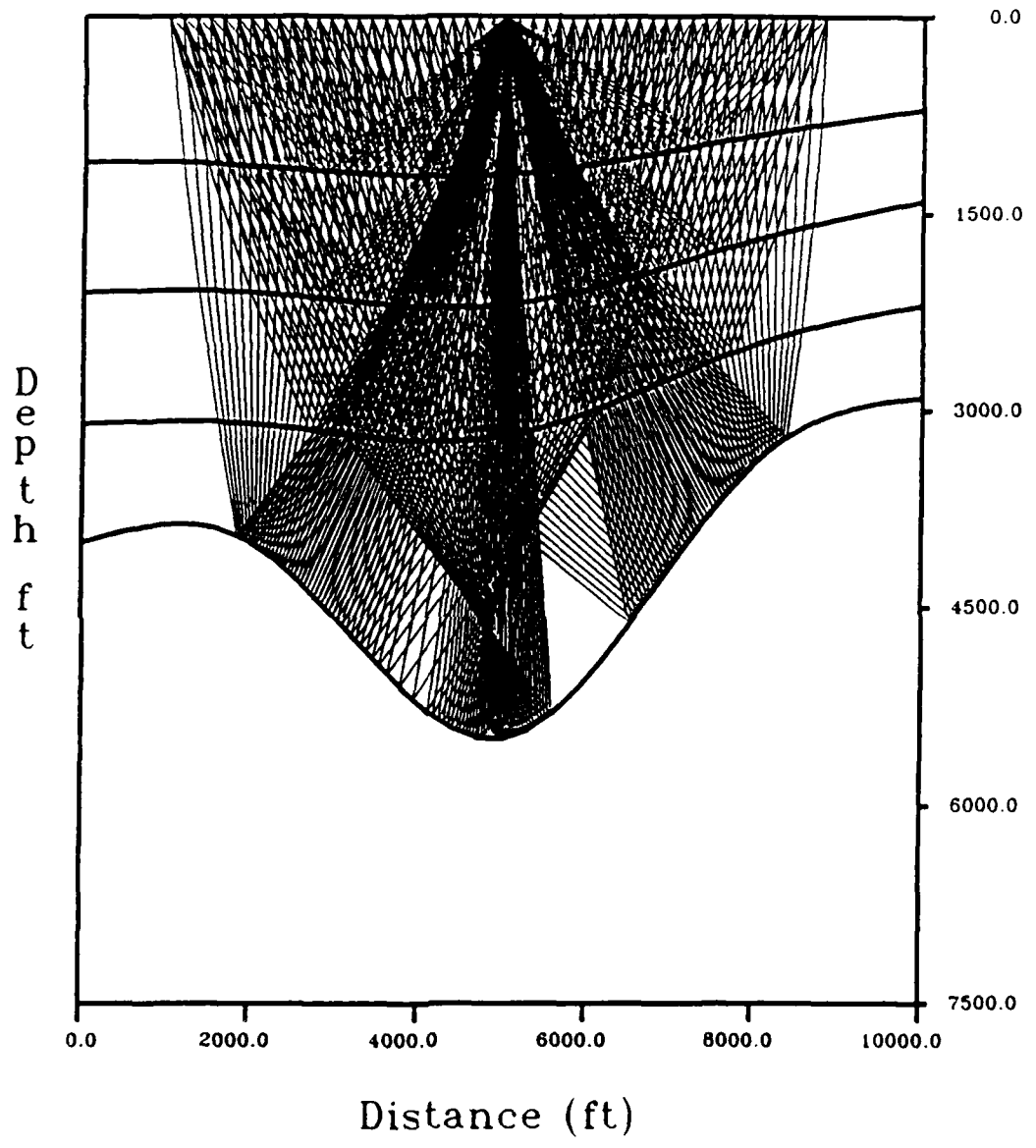


Figure 1

Cshot Data of A Syncline

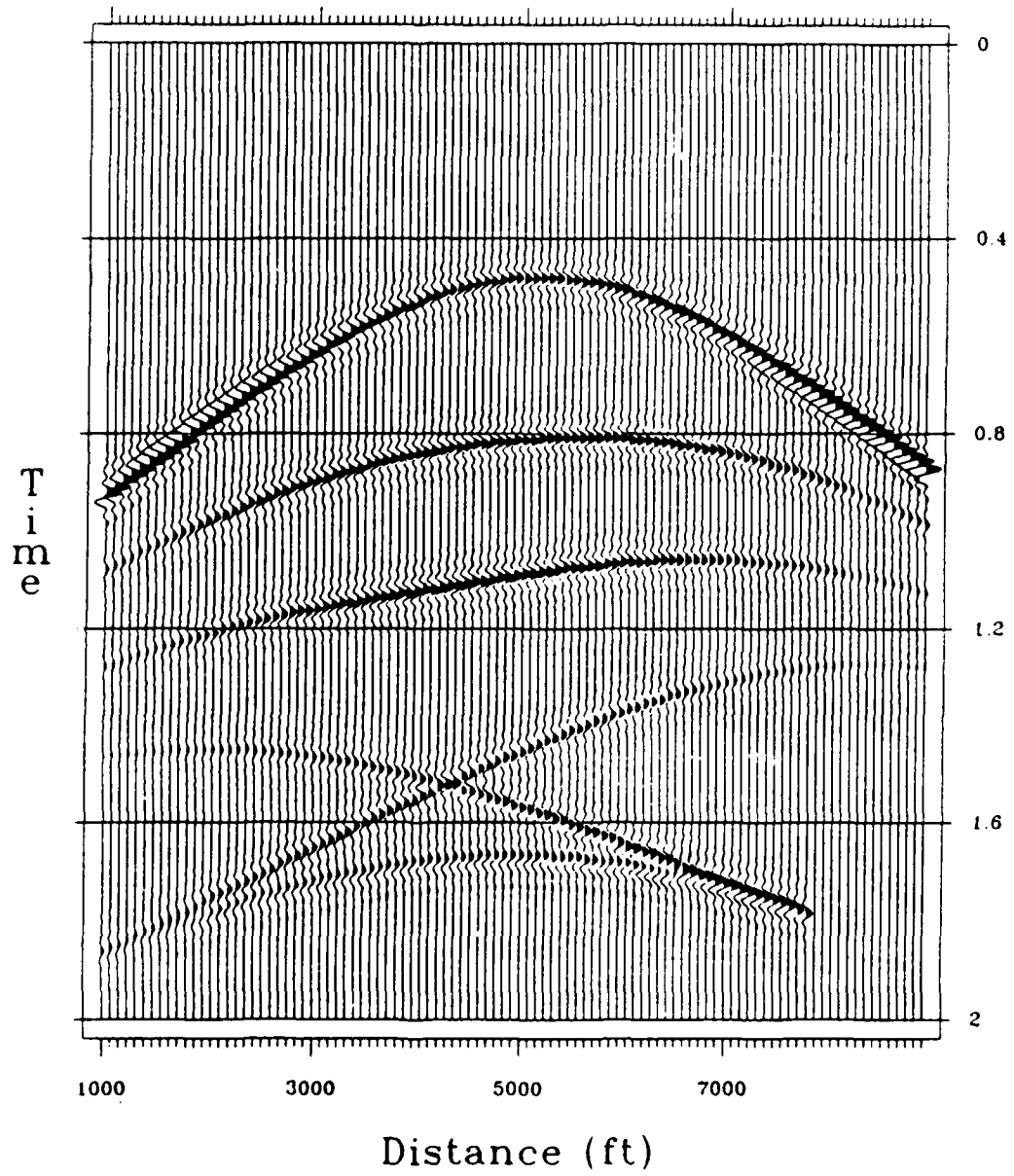


Figure 2

Syncline Inversion

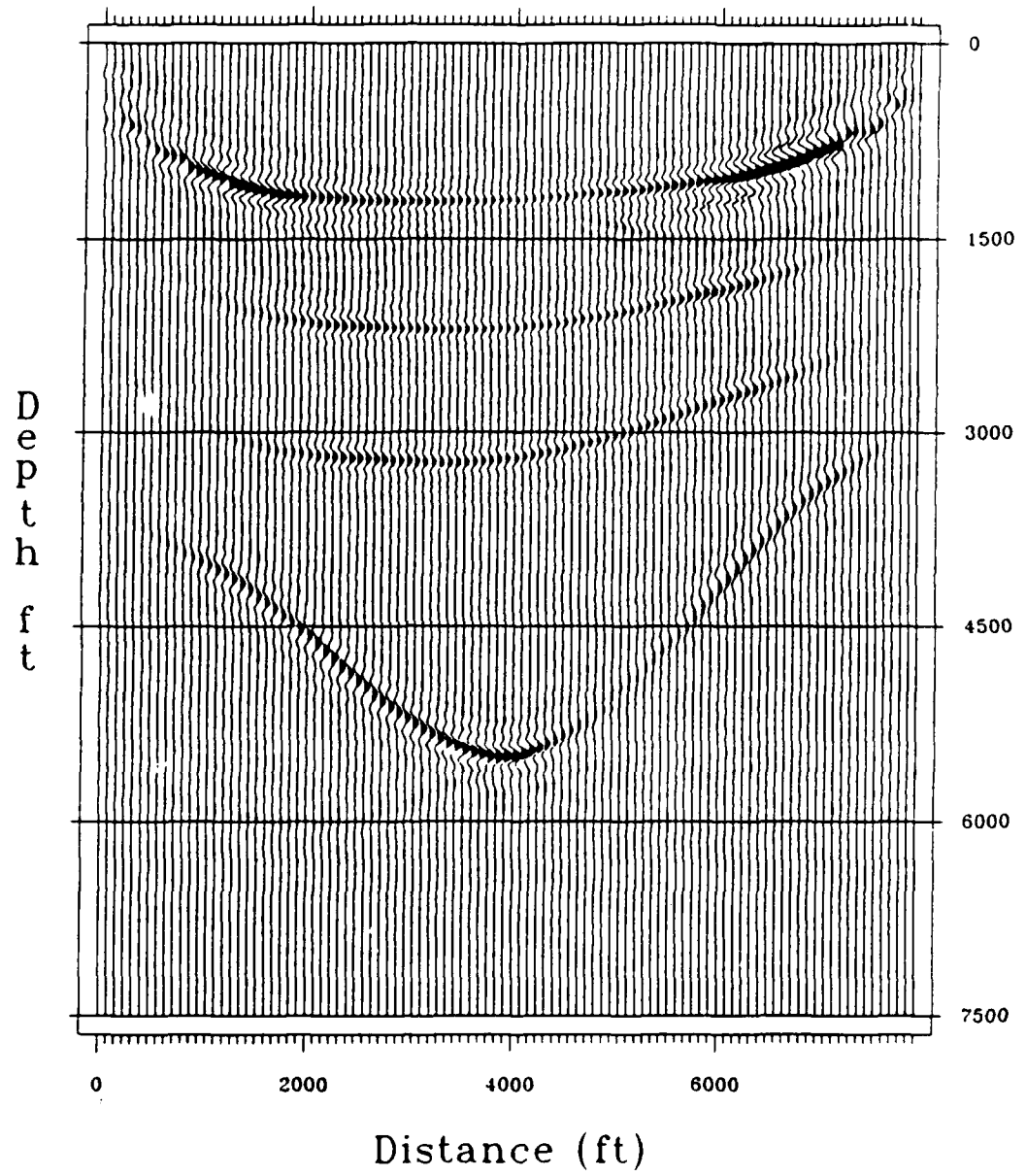


Figure 3

Marathon Data Model

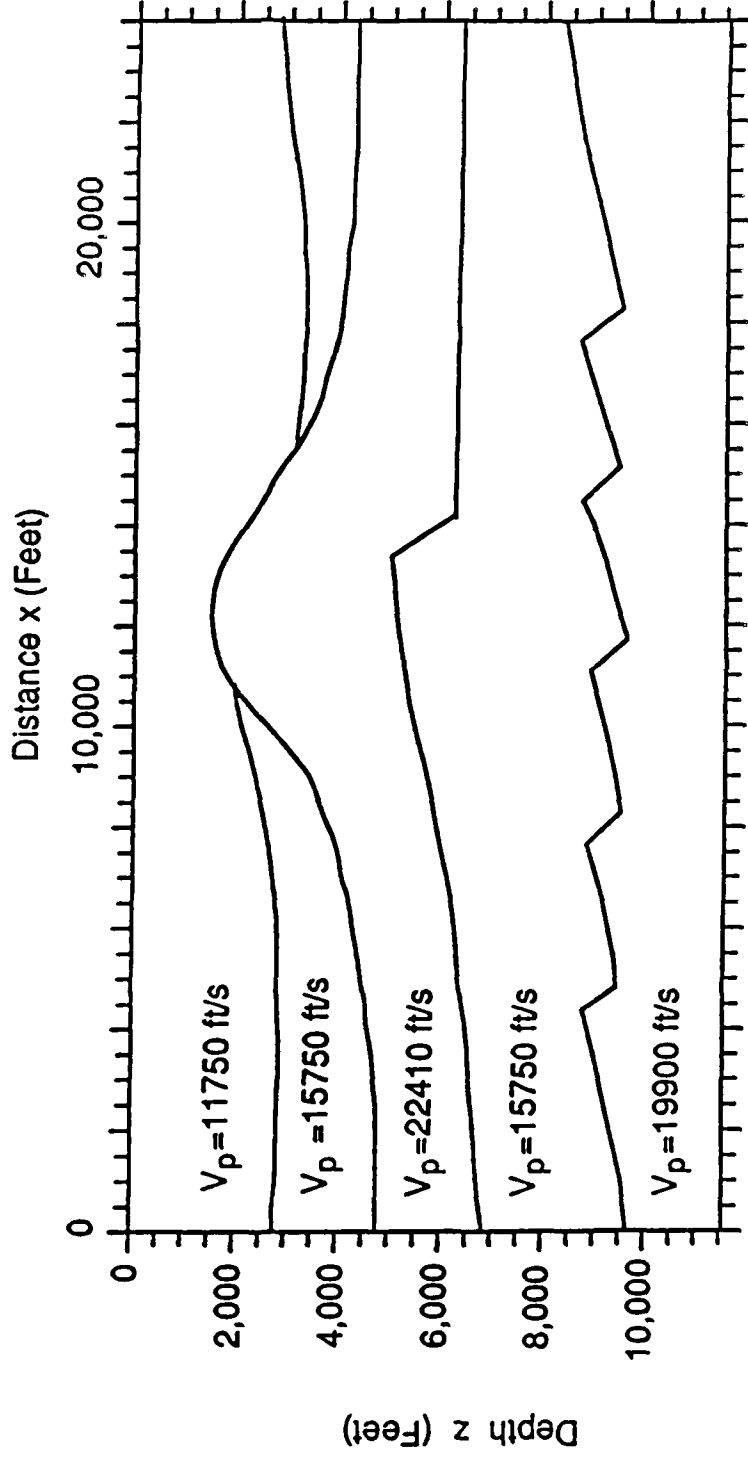


Figure 4

Shot 2000

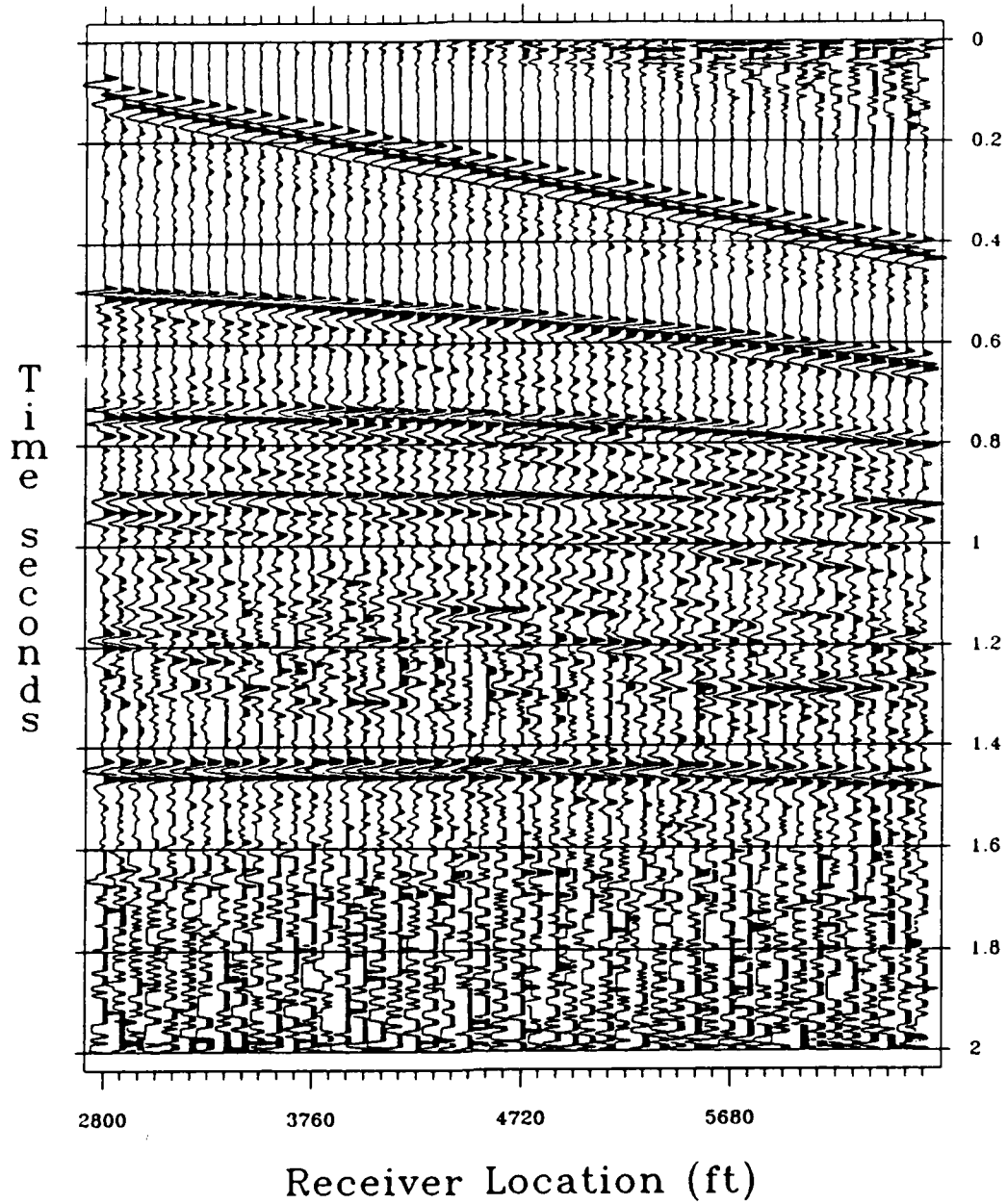


Figure 5

Inversion of Shot 20000

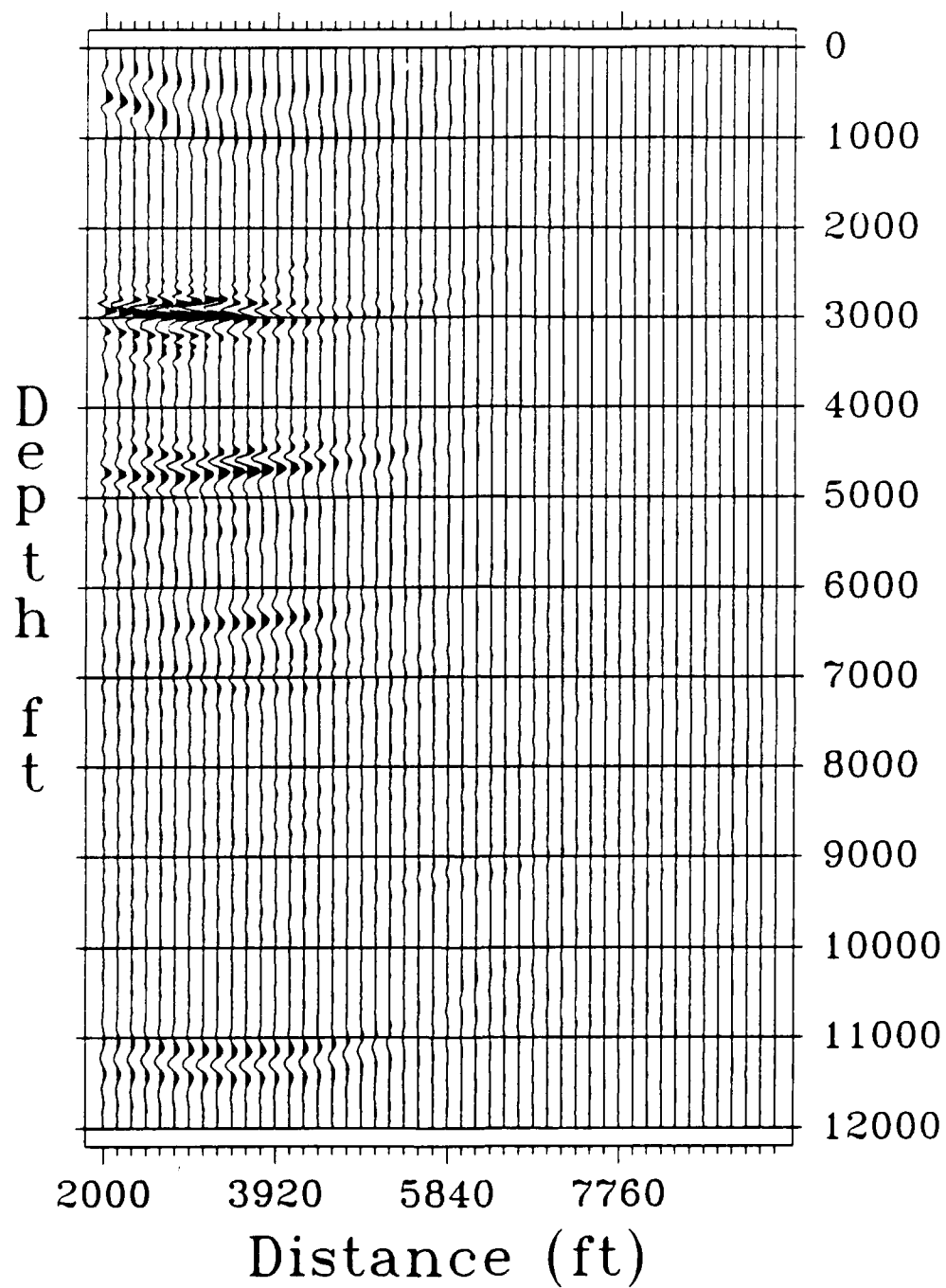


Figure 6

Stack of All Inversions (gained)

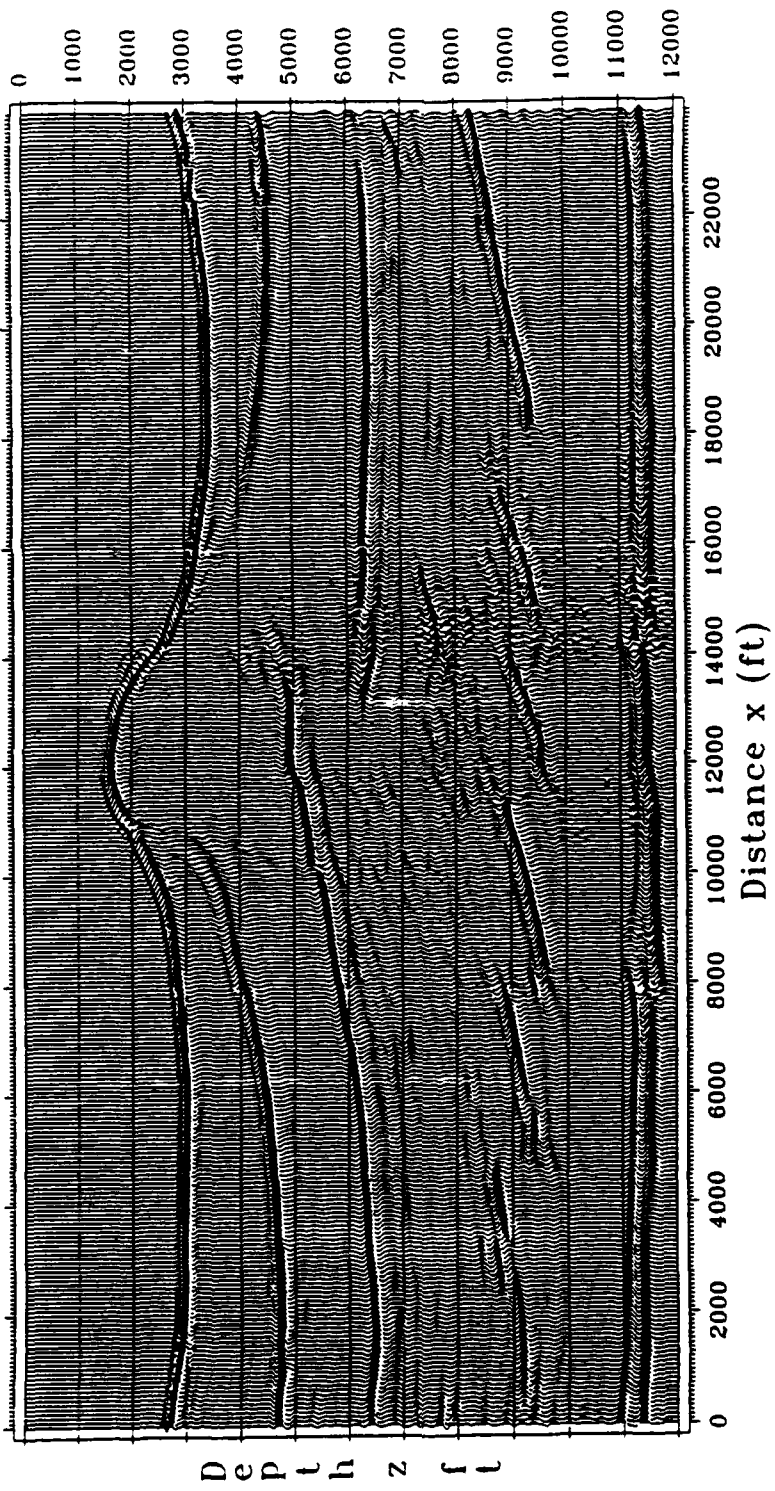


Figure 7

Stack of All Shot Inversions (gained)

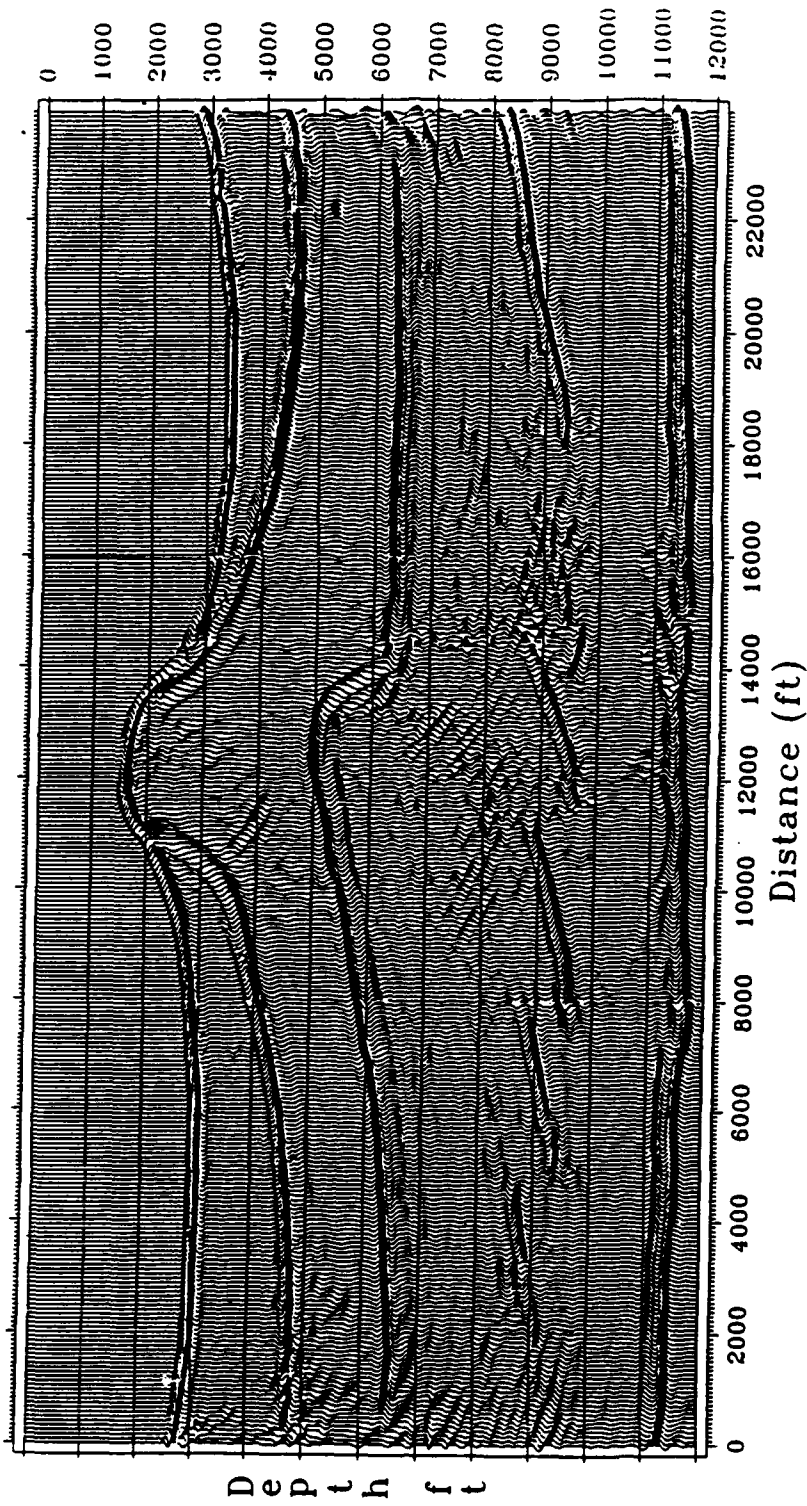


Figure 8



Figure 9



Figure 10

REPORT DOCUMENTATION PAGE

1a REPORT SECURITY CLASSIFICATION Unclassified			1b RESTRICTIVE MARKINGS None			
2a SECURITY CLASSIFICATION AUTHORITY			3 DISTRIBUTION/AVAILABILITY OF REPORT			
2b DECLASSIFICATION/DOWNGRADING SCHEDULE						
4 PERFORMING ORGANIZATION REPORT NUMBER(S) CWP-090P			5 MONITORING ORGANIZATION REPORT NUMBER(S)			
6a NAME OF PERFORMING ORGANIZATION Center for Wave Phenomena Colorado School of Mines		6b OFFICE SYMBOL (if applicable)	7a NAME OF MONITORING ORGANIZATION Mathematical Sciences Division Office of Naval Research			
6c ADDRESS (City, State, and ZIP Code) Golden, CO 80401			7b ADDRESS (City, State, and ZIP Code) 800 N. Quincy Street Arlington, VA 22217-5000			
8a NAME OF FUNDING/SPONSORING ORGANIZATION		8b OFFICE SYMBOL (if applicable)	9. PROCUREMENT INSTRUMENT IDENTIFICATION NUMBER N00014-88-K-0092			
8c ADDRESS (City, State, and ZIP Code)			10. SOURCE OF FUNDING NUMBERS			
			PROGRAM ELEMENT NO.	PROJECT NO.	TASK NO.	WORK UNIT ACCESSION NO.
11 TITLE (Include Security Classification) A Computer Implementation of 2.5D Common Sh h et Inversion						
12 PERSONAL AUTHOR(S) Wenjie Dong, M.J. Emanuel, P. Bording, N. Bleistein						
13a TYPE OF REPORT Technical		13b TIME COVERED FROM _____ TO _____		14 DATE OF REPORT (Year, Month, Day) June 1990	15 PAGE COUNT 44	
16 SUPPLEMENTARY NOTATION Submitted for publication in <u>Geophysics</u> .						
17 COSATI CODES			18. SUBJECT TERMS (Continue on reverse if necessary and identify by block number)			
FIELD	GROUP	SUB-GROUP				
19 ABSTRACT (Continue on reverse if necessary and identify by block number) See reverse side.						
20 DISTRIBUTION/AVAILABILITY OF ABSTRACT <input checked="" type="checkbox"/> UNCLASSIFIED/UNLIMITED <input type="checkbox"/> SAME AS RPT <input type="checkbox"/> DTIC USERS			21. ABSTRACT SECURITY CLASSIFICATION			
22a NAME OF RESPONSIBLE INDIVIDUAL Norman Bleistein			22b TELEPHONE (Include Area Code) (303)273-3557	22c. OFFICE SYMBOL		

ABSTRACT

This paper describes the computer implementation of a two-and-one-half dimensional (2.5D) constant density prestack inversion formalism with laterally and depth-dependent background propagation speed. This is a Kirchhoff-type inversion, summing a line of receiver data over traveltimes in the depth-dependent background medium with weights determined from the Born/Kirchhoff inversion theory. This theory predicts that the output will be a reflector map with peak amplitudes on each reflector being in known proportion to the angularly dependent geometrical optics reflection coefficient. The 2.5D feature provides for out-of-plane spreading correction consistent with the prescribed background medium. The method is applied to a synthetic data set and to an experimental data set generated at the Seismic Acoustic Laboratory at the University of Houston under support of the Marathon Oil Company. The graphical output demonstrates the validity of the formalism as a Kirchhoff migration. Parameter estimation for the experimental data was less successful, partially due to problems with amplitude control in the original experiment and partially due to the limited aperture of the common shot data, thereby suggesting that a common offset inversion might be more useful for parameter estimation. This paper is primarily based on the master's theses projects of the first two authors.